

Crystallization behavior and characteristics of mullites formed from alumina–silica gels prepared by the geopolymer technique in acidic conditions

T. Iwahiro, Y. Nakamura, R. Komatsu, K. Ikeda*

Department of Advanced Materials Science and Engineering, Yamaguchi University, Ube 755-8611, Japan

Abstract

Mullites were prepared by the geopolymer technique to obtain nanometer sized mullite polycrystals. Sodium silicate solutions prepared from $\text{Na}_2\text{O}\cdot\text{SiO}_2\cdot 9\text{H}_2\text{O}$ (A-series) and $\text{Na}_2\text{O}\cdot 2\text{SiO}_2\cdot \text{aq}$ (B-series) were applied as host solutions. Then, Al-nitrate guest solution was added drop by drop into the host solutions to obtain precipitates, which were filtrated and washed by deionized water. The air-dried precursor gels thus obtained were fired at elevated temperature up to 1400°C and were examined by XRD, DTA and ICP techniques. The XRD results showed that the A-series gels began to crystallize mullite at about 1000°C , while the B-series at about 1100°C . According to the DTA, a sharp exothermic peak appeared at about 1000°C in the A-series gels indicating polymer character of the gels, while no such a peak in the B-series gels indicating nonpolymer character of the gels. Chemical analysis by ICP revealed low concentration of Al_2O_3 -component in the gels, and this caused the gels consisted of mullite and silica potentials. Na-contaminations were extremely low. The process of mullite generation was also discussed on the basis of cell-parameters measured. © 2001 Elsevier Science Ltd. All rights reserved.

Keywords: AlN; Mullite; Sol-gel processes

1. Introduction

Mullite has been widely used as refractories because of the high melting point ($\sim 1890^\circ\text{C}$), the high creep resistance and the high thermal shock resistance. Recently, the application fields of mullite have been expanding not only to aircraft engines but also to IC substrates in electronics, catalyst supports in automobiles and so on.^{1,2} Therefore, fine grained and high purity mullite powders are requested in order to obtain fully dense mullite ceramics. In this objective, sol-gel technique has been widely used.³ However, there may be some disadvantage of cost performance and so on in this technique. In this paper another novel technique called the geopolymer technique will be studied. The geopolymer technique developed by Davidovits⁴ was initially applied for preparation of monolithic materials, starting from meta-kaolin and reactive silica under the presence of strong alkaline solutions such as KOH at 80°C . Recently this processing temperature was improved down to room temperature by direct application of alkaline silicate solutions, i.e. water glasses.⁵ Studying polycondensation

mechanism of $[\text{SiO}_4]$ -monomers is now becoming urgent to solve for this technique. Therefore, the second objective of this study is to reveal polycondensation mechanism in geopolymer systems.

2. Experimental

Reagent grade chemicals of metasilicate, $\text{Na}_2\text{O}\cdot\text{SiO}_2\cdot 9\text{H}_2\text{O}$ and honey type disilicate, $\text{Na}_2\text{O}\cdot 2\text{SiO}_2\cdot \text{aq}$ were diluted with deionized water to obtain host solutions for SiO_2 -sources labeled A and B, respectively. Al-nitrate nonahydrate, $\text{Al}(\text{NO}_3)_3\cdot 9\text{H}_2\text{O}$ was also diluted with deionized water to obtain guest solution labeled C for Al_2O_3 -source. Specifications of these starting solutions are listed in Table 1 together with mixing proportions. The guest solution C was added drop by drop into the host solution, A or B with various mixing conditions (Table 1). After pH measurements followed by 2 h standing time, the precipitates were filtrated and washed several times by deionized water and dried at room temperature. The dried precursor gels were fired at elevated temperatures from 900 to 1400°C with 50 – 100°C intervals for 1 h. Crystallization behavior and crystalline phases obtained were examined by XRD and DTA. The crystallite size of the mullite was calculated using

* Corresponding author. Tel.: +81-836-85-9630; fax: +81-836-85-9601.

E-mail address: k-ikeda@po.cc.yamaguchi-u.ac.jp (K. Ikeda).

Table 1
Concentration and mixing proportion of starting solutions

Solution A	Na-metasilicate, $\text{Na}_2\text{O}\cdot\text{SiO}_2\cdot 9\text{H}_2\text{O}$	S.G. ^a 1.13(1.07) ^b mol/l
Solution B	Na-disilicate, $\text{Na}_2\text{O}\cdot 2\text{SiO}_2\cdot \text{aq}$	1.27(1.48)
Solution C	Al-nitrate solution, $\text{Al}(\text{NO}_3)_3\cdot 9\text{H}_2\text{O}$	1.38(1.00)

Mixing proportion

A-series (A:C) 1:1, 1:2, and 1:3 in volume

B-series (B:C) 1:1, 1:2, and 1:3 in volume

^a S.G.: specific gravity

^b Concentration of dry-base Na-silicates corresponding to liquor.

the Scherrer equation, measuring peak width of (121) reflection profiles. The chemical compositions of gels were analyzed by the ICP technique. The unit-cell parameters of the mullite were determined by the least squares method, employing Mac Sience X-ray diffractometer, MXP3, equipped with an automatic centering system of the goniometer under following conditions: 40 kV–20 mA CuK_α radiation with graphite monochromator, 0.02° step scan and 3 s counting time, and $1^\circ(\text{DS})\text{--}1^\circ(\text{SS})\text{--}0.15$ mm (RS) slit system.

3. Results and discussion

3.1. XRD

The samples obtained were amorphous and began to crystallize mullite with elevation of heating temperature as shown in Fig. 1. It was found that the A-series gels began to crystallize at about 1000°C and relatively high-crystalline state was reached over 1100°C , while the B-series gels began to crystallize at about 1100°C and relatively high-crystalline state over 1200°C , noting (121) reflections at 40.9° , 2θ . The A-series gel prepared by mixing A:C=1:1 showed slightly higher mullitization temperature, probably due to the higher content of alumina component (Table 4). Crystallization of cristobalite was observed by heating over 1300°C in the B-series

gels, but was unclear and trace in the A-series gels. The crystalline phases observed are summarized in Table 2.

3.2. DTA

As shown in Fig. 2, the DTA curves were characterized by the first endothermic peak of dehydration centered at about 120°C irrespective of mixing proportions. At elevated temperatures, however, sharp exothermic peaks were observed around 1000°C in the A-series gels, while no exothermic in the B-series gels even at elevated temperatures over 1000°C which were omitted in Fig. 2. This suggests that the A-series gels are in polymerized state in atomic order as generally seen in glass devitrification

Table 2
Crystalline phases after firing the precursors

$^\circ\text{C}$	A-series			B-series		
	1:1	1:2	1:3	1:1	1:2	1:3
1400	M	M	M	M, C ^a	M, C	M, C
1300	M	M	M	M, C	M, C	M
1200	M	M	M	M	M	M
1150	M	M	M	M	M	M
1100	M	M	M	M	M	M
1050	M	M	M	–	–	–
1000	–	M	M	–	–	–
900	–	–	–	–	–	–

^a M, mullite; C, cristobalite.

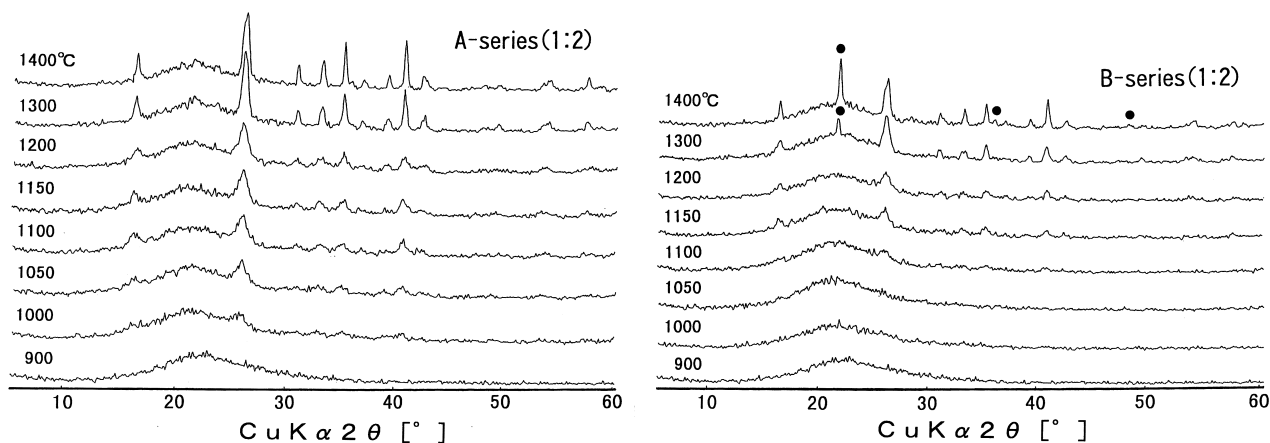


Fig. 1. XRD results for A- and B-series precursors. Here only cristobalite peaks are indicated with solid circles and other peaks are of mullite.

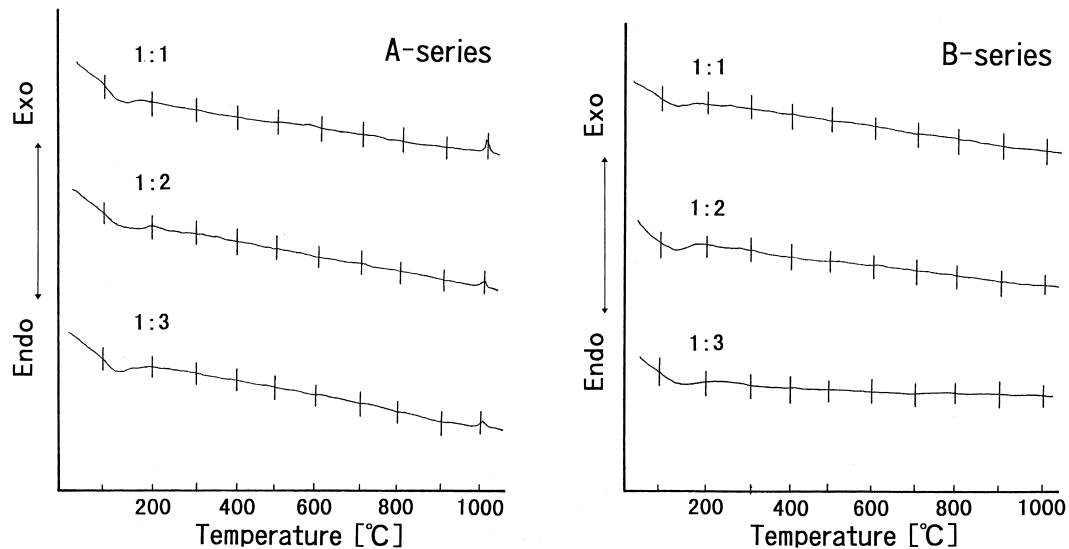


Fig. 2. DTA results for A- and B-series precursors.

as well as hydrous mineral transformation to dry minerals in the course of heating.⁶ On the contrary, the B-series gels are composed of aggregates of precipitated gels made up of hydrous silica and alumina.

Judging from the XRD results in Fig. 1, the observed exothermic peaks for the A-series may only indicate nucleation of mullite embryos from the amorphous precursor gels, and then crystal growth may proceed gradually to provide clear XRD charts with elevation of heating temperature. In liebenbergite gels consisting of Ni_2SiO_4 -olivine and cristobalite potentials, an instant crystallization from polymer gels were observed, showing clear XRD charts from the beginning irrespective of heating temperature over exothermic peaks.⁷ Therefore, slightly different gel characters are considered between the present A-series gels and the liebenbergite gels in polymerized state.

The B-series gels may have short range order structures consisting of simple hydrous precipitate mixtures, because they do not show exothermic peaks at all. In other words, the B-series gels may be coprecipitates of hydrous silica and alumina mixtures and may crystallize into mullite and cristobalite only through reaction sintering as usually seen in powdered oxide starting materials.

3.3. Crystallite size

As tabulated in Table 3, nanometer sized crystallites were obtained irrespective of the starting gels. Although slightly larger size was noted in the B-series gels than in the A-series gels, the difference was not so marked. With elevation of heating temperature significant growth of crystallite was observed in size. Therefore, it can be said that formation of fine grained mullite at high temperatures are independent of atomic order polymerization, if the starting solid grains are sufficiently small. The

Table 3
Crystallite size (nm) of mullites

°C	A-series			B-series		
	1:1	1:2	1:3	1:1	1:2	1:3
1400	29	34	33	36	36	37
1300	22	26	20	29	23	22
1200	17	15	16	18	22	17

B-series gels considered to be finely mixed aggregates of precipitates can also produce fine grained mullites.

3.4. Chemical composition

As tabulated in Table 4, the gels prepared had low quantity of Al_2O_3 -component, ranging from 29.00 to 36.51 wt.% in the A-series gels and from 19.53 to 20.96 wt.% in the B-series gels. The ideal quantity of alumina component should be 71.80 and 77.24 wt.% for 3/2- and 2/1-mullites, respectively. Therefore, the analyzed chemical compositions are suggesting the potential of silica-rich phases in the heated gels other than mullite, most probably cristobalite.

Table 4
Dry-base chemical compositions of gels (wt.%) and pH before filtration

	pH	SiO_2	Al_2O_3	Na_2O
<i>A-series</i>				
1:1	3.6	63.24	36.51	0.25
1:2	2.8	68.21	31.55	0.24
1:3	2.5	70.89	29.00	0.11
<i>B-series</i>				
1:1	2.3	78.48	20.96	0.56
1:2	1.7	80.15	19.72	0.13
1:3	1.4	80.14	19.53	0.33

There was a tendency of enrichment of alumina in the gels, especially in the A-series, depending on mixing proportions from 1:3 to 1:1. The pH values measured suggest that extremely low pH of the solution is inconvenient to obtain gels including more alumina-component. This is due to the high solubility of alumina-component in acidic solutions. As a consequence, the optimum pH was 3.6 corresponding to the 1:1 solution of the A-series in this experiment, but the Al_2O_3 content was only 36.51 wt.%.

The residual sodium contents in the gels were extremely lower than those expected and were 0.11–0.25 wt.% range in the A-series, while 0.13–0.56 wt.% range in the B-series, both as Na_2O . It is estimated that polycondensed molecules are mainly terminated with hydroxyls, $-\text{OH}$ instead of $-\text{ONa}$ in the A-series gels. On the contrary, as mentioned in the DTA section, the B-series gels would form as simple coprecipitates consisting of hydrous silica and alumina mixtures which were contaminated with a slight sodium adsorption. Consequently, sodium component being present enormously in the starting solutions almost remained in the

supernatants and excluded from the obtained gel samples. We found, however, significantly high sodium contamination in a gel precursor of liebenbergite, Ni_2SiO_4 , and cristobalite, being 5.95 wt.% as Na_2O , when based on dry-base.⁷ This Ni-bearing precursor was polymer character of diphasic gel showing instant crystallization after double exothermic peaks around 800°C in the DTA chart, attributed to liebenbergite and cristobalite crystallization occurring so instant. Consequently, abundance of $-\text{ONa}$ termination was considered for this Ni-bearing gel.

3.5. Cell-parameter

Cell-parameters measured are plotted in Fig. 3 in terms of cell volume versus c -axis dimension, both are determinable relatively in high precision as summarized in Table 5. This diagram was cited from literature⁸ and was revised slightly. It has been pointed out that there are two distinct trends in this diagram. One is the linear trend extending from 3/2-mullite to 2/1-mullite. The other is the nonlinear trend applicable to Fe, Ti-bearing mullites.

The results in this study exhibit that there are two groups of mullite prepared by the geopolymer technique. One is the larger c -axis group plotted in relatively wide area. The other is the smaller c -axis group plotted near the 3/2- to 2/1-mullite line. Therefore, we are now considering that the first group, i.e. low crystallinity group, might be metastable mullites recrystallized from the mullites initially crystallized out at lower temperatures, while the second group, i.e. high crystallinity group, might be stable mullites reconstructed from the metastable mullite at higher temperatures. From this diagram it is expected that specimens A13(1:1) and B14(1:1) heated at 1300 and 1400°C, respectively, should be plotted in the metastable and the stable regions, respectively, but they showed exceptional behavior, probably due to their crystallinity resulted depending on

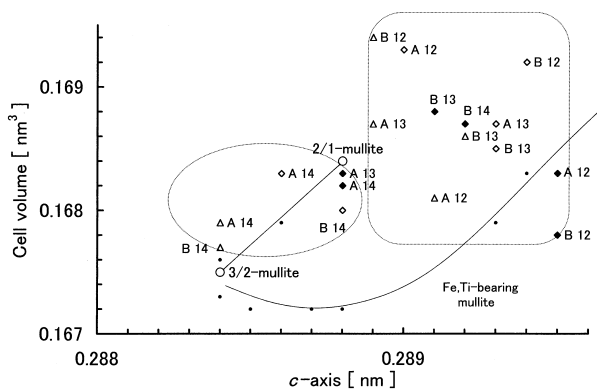


Fig. 3. Obtained mullite classification in terms of cell-volume versus c -axis dimension. Specimen notation, \blacklozenge (1:1), \diamond (1:2), Δ (1:3) common to A- and B-series and numerals indicating temperature of formation; $\times 100$. Small solid circles representing the original literature data.⁸

Table 5
Detailed representation of cell-parameters of mullites^a

	1200°C			1300°C			1400°C		
	1:1	1:2	1:3	1:1	1:2	1:3	1:1	1:2	1:3
<i>A-series</i>									
a_0 (nm)	0.7612 (11)	0.7623 (11)	0.7591 (8)	0.7566 (7)	0.7571 (7)	0.7561 (5)	0.7556 (4)	0.7560 (3)	0.7563 (5)
b_0 (nm)	0.7668 (7)	0.7687 (13)	0.7659 (9)	0.7704 (2)	0.7703 (7)	0.7719 (5)	0.7707 (5)	0.7714 (4)	0.7649 (5)
c_0 (nm)	0.2895 (2)	0.2890 (3)	0.2891 (2)	0.2888 (2)	0.2886 (2)	0.2890 (2)	0.2888 (2)	0.2893 (1)	0.2884 (2)
V (nm ³)	0.1681 (0)	0.1694 (3)	0.1681 (2)	0.1683 (2)	0.1683 (2)	0.1683 (2)	0.1682 (1)	0.1687 (1)	0.1679 (2)
<i>B-series</i>									
a_0 (nm)	0.7535 (12)	0.7583 (17)	0.7595 (11)	0.7576 (5)	0.7589 (6)	0.7577 (8)	0.7560 (9)	0.7548 (4)	0.7549 (2)
b_0 (nm)	0.7690 (9)	0.7721 (10)	0.7717 (9)	0.7709 (4)	0.7690 (8)	0.7695 (10)	0.7717 (11)	0.7705 (3)	0.7701 (3)
c_0 (nm)	0.2895 (3)	0.2894 (3)	0.2890 (3)	0.2891 (2)	0.2894 (2)	0.2893 (3)	0.2892 (3)	0.2889 (1)	0.2884 (0)
V (nm ³)	0.1678 (3)	0.1694 (3)	0.1693 (3)	0.1689 (1)	0.1682 (2)	0.1687 (2)	0.1687 (3)	0.1680 (1)	0.1679 (1)

^a Standard deviation in parentheses.

polymer and nonpolymer characters as detected by DTA. It is of interest to note that B14(1:3) having relatively lower alumina content finally reached near the 3/2-mullite point, while A13(1:1) and A14(1:1) both having relatively higher alumina content finally reached near 2/1-mullite point. The finally crystallized mullites of others were plotted on intermediate points between the 3/2- and 2/1-mullite line, but strong deviations from the trend line was noted.

4. Conclusion

1. Polymerized mullite precursors can be prepared from $\text{Na}_2\text{O}\cdot\text{SiO}_2$ solutions rather than from $\text{Na}_2\text{O}\cdot 2\text{SiO}_2$ solutions.
2. Mullite crystallization occurs around 1000°C , when $\text{Na}_2\text{O}\cdot\text{SiO}_2$ solutions are applied, while that is around 1100°C , slightly higher, when $\text{Na}_2\text{O}\cdot 2\text{SiO}_2$ solutions are applied.
3. Nanometer sized mullite powders can be prepared irrespective of starting water glass solutions, meta-silicate or disilicate. The crystallites are dependent on heating temperatures in size as summarized in Table 3, ranging from tens to thirties of nm.
4. Sodium contamination is low, ranging 0.11–0.25% and 0.13–0.56% for the $\text{Na}_2\text{O}\cdot\text{SiO}_2$ and $\text{Na}_2\text{O}\cdot 2\text{SiO}_2$ solutions, respectively.
5. Obtained mullites from the gels can be classified into two groups, one has larger c -axis dimension

peculiar to low crystalline mullites generally formed at low temperatures and the other has smaller c -axis dimension peculiar to high crystalline mullites formed at higher temperatures.

6. At the moment, single phase mullite has not been obtained yet is always associated with cristobalite being crystalline or amorphous.

References

1. Schneider, H., Okada, K. and Pask, J., *Mullite and Mullite Ceramics*. John Wiley, Chichester, 1994.
2. Katsuki, H., Furuta, S. and Komarneni, S., Formation of novel ZSM-5-porous mullite composit from sintered kaolin honeycomb by hydrothermal reaction. *J. Am. Ceram. Soc.*, 2000, **83**, 1093–1097.
3. Schneider, H., Ikeda, K., Saruhan, B. and Rager, H., Electron paramagnetic resonance and optical absorption studies on Cr-doped mullite. *J. Eur. Ceram. Soc.*, 1996, **16**, 211–215.
4. Davidovits, J., *Mineral Polymers and Method of Making Them* US patent, 4349386, 14 September 1982.
5. Ikeda, K., Consolidation of mineral powders by the geopolymer binder technique for materials use. *Shigen-to-Sozai*, 1998, **114**, 497–500 (in Japanese).
6. Sasaki, K., Masuda, T., Ishida, H. and Mitsuda, T., Synthesis of calcium silicate hydrate with $\text{Ca}/\text{Si}=2$ by mechanochemical treatment. *J. Am. Ceram. Soc.*, 1977, **80**, 472–476.
7. Ikeda, K., Onikura, K., Nakamura, Y. and Vedanand, S., Optical spectra of Ni-bearing silicate gels prepared by the geopolymer technique with special reference to the low temperature formation of liebenbergite, Ni_2SiO_4 . *J. Am. Ceram. Soc.* in press.
8. Agrell, S. O. and Smith, J. V., Cell dimensions, solid solution, polymorphism and identification of mullite and silimanite. *J. Am. Ceram. Soc.*, 1960, **43**, 69–76.